Optical Pump-Probe Measurements of Local Nuclear Spin Coherence in Semiconductor Quantum Wells

H. Sanada,[1] Y. Kondo,[1] S. Matsuzaka,[1] K. Morita,[2,1] C. Y. Hu,[1,3] Y. Ohno,[1,3,*] and H. Ohno[1,2,†]

[1]*Laboratory for Nanoelectronics and Spintronics, Research Institute of Electrical Communication, Tohoku University, Katahira 2-1-1, Aoba-ku, Sendai 980-8577, Japan*
[2]*ERATO Semiconductor Spintronics Project, Japan Science and Technology Agency, Japan*
[3]*CREST, Japan Science and Technology Agency, 6-17-9 Hongo, Bunkyo-ku, Tokyo 113-0033, Japan*
(Received 22 August 2005; published 17 February 2006)

We demonstrate local manipulation and detection of nuclear spin coherence in semiconductor quantum wells by an optical pump-probe technique combined with pulse rf NMR. The Larmor precession of photoexcited electron spins is monitored by time-resolved Kerr rotation (TRKR) as a measure of nuclear magnetic field. Under the irradiation of resonant pulsed rf magnetic fields, Rabi oscillations of nuclear spins are traced by TRKR signals. The intrinsic coherence time evaluated by a spin-echo technique reveals the dependence on the orientation of the magnetic field with respect to the crystalline axis as expected by the nearest neighbor dipole-dipole interaction.

Nuclear magnetic resonance (NMR) [1] is widely used to analyze structures and electronic states in a variety of materials. In addition, NMR has been highlighted as a key technology to implement quantum information processing [2]. It is one of the most challenging but fascinating targets for the current science and technology to realize quantum computing devices, for which nuclear spins in semiconductor nanostructures have attracted great interest as a scalable media of quantum information manipulation and storage [3–5]. Also a number of experimental studies have revealed that nuclear spins play crucial roles in spin-dependent electrical and optical properties of semiconductor quantum wells (QWs) [6–8] and quantum dots (QDs) [9–11], the understanding of which is essential for novel spintronic devices. In this context, much effort has been devoted to exploit a new class of NMR techniques with extremely high sensitivity and nanometer-scale resolution. Sensitivity of NMR can be improved orders of magnitude by enhancing nuclear polarization through the contact hyperfine interaction with nonequilibrium spin polarized electrons, which can be optically prepared by irradiation of circularly polarized light [12,13]. In addition to using a conventional pickup coil [14], optical detection of cw-NMR has been demonstrated by using probes that reflect the local nuclear magnetic field acting on the electron spins, such as luminescence polarization [15–17], which is limited by the radiative charge recombination time, or Faraday and Kerr rotation [18,19], which can be used for a much broader time scale.

Detection by optical means is suitable for local detection of nuclear spin dynamics, especially because the area of which can be defined by the extent of the electron distribution that responds to the optical field [7]. However, there have been only a few reports in which the coherent feature of nuclear spins is observed by optical detection; in all the cases luminescence was used, in a heterostructure [20] and for a nitrogen-vacancy defect in diamond [21]. Recently, instead, electrical detections of quantum coherence in NMR have been demonstrated in Hall-bar [22] and point-contact [23] devices formed on a GaAs/(Al, Ga)As two-dimensional electron (2DE) system with a planar rf antenna. These approaches, however, can work only under the conditions restricted to particular quantum Hall states.

Here we employed an optical pump-and-probe technique for the observation of nuclear spin coherence in semiconductor QWs, where efficient dynamic nuclear polarization can be achieved by optically excited 2DE spins almost transverse to the applied magnetic fields [6]. In the following, we present an optical detection of spin echo and evaluate the intrinsic phase coherence time T_2 of constituent nuclei by time-resolved Kerr rotation (TRKR) combined with pulse rf NMR.

The sample we studied here was grown on a (110)-oriented semi-insulating GaAs substrate by molecular beam epitaxy. It consists of 5 periods of 7.5 nm-thick GaAs QWs with nominal Si donor density of 6×10^{17} cm^{-3} (4.5×10^{11} cm^{-2} per each QW), each of which is separated by a 10 nm-thick undoped $Al_{0.3}Ga_{0.7}As$ barrier. The wafer was cleaved to a 5 mm $\times$ 5 mm piece and set in a cryostat with a superconducting magnet. In the TRKR measurements, we used a mode-locked Ti:sapphire laser with a pulse duration of 110 fs and repetition rate of 76 MHz. The photon energy was tuned at the resonant excitation of the lowest electron-heavy hole absorption peak. The pulse train derived from the laser was divided into pump pulses (circularly polarized) and probe pulses (linearly polarized), and their relative delay time Δt was varied using a mechanical delay line. The pump- and probe-beam powers were set at 5 and 0.5 mW, respectively. The diameter of the spot size was 40 μm on the sample,

within which we observe an ensemble of the dynamics of roughly $\sim 10^{12}$ nuclear spins. The Kerr rotation angle θ_K of the reflected probe beam was measured by using a balanced detector with a resolution of 10 mdeg.

Our NMR setup is schematically shown in Fig. 1(a). rf magnetic field $\boldsymbol{B}_{rf}$ is applied to the sample by a split-coil wound around the sample. For impedance matching and induction of higher $\boldsymbol{B}_{rf}$ at resonance, a capacitor is connected in series: the rf power of ~ 100 W at the resonant frequency $f_{rf} = 8.18$ MHz is fed to the LC resonator through a semirigid coaxial cable. The directions of $\boldsymbol{B}_{rf}$, incident laser beams, and external static magnetic field $\boldsymbol{B}$ are taken along the x, y, and z axis, respectively. The sample was set so that the $[1\bar{1}0]$ direction is along the x axis, while the $[001]$ direction in the (110) QW plane is tilted by an angle α with respect to the z axis to enhance dynamic nuclear polarization [6] as well as to control the nuclear dipole-dipole interaction as described later. The sample temperature was kept at 5.5 ± 0.1 K throughout the experiments [24].

Upon irradiation of circularly polarized pump pulses and application of $\boldsymbol{B}$ greater than the threshold field for dynamic nuclear polarization (several tens of mT [25]), nuclear spin polarization is enhanced by the Overhauser effect, and in a time scale of ~ 100 s it reaches a steady

state in balance with time-averaged electron spin polarization. The degree of the nuclear polarization can be evaluated from the Larmor precession frequency ν_L of the electron spins, which is given by a sum of the Zeeman splitting and the hyperfine coupling as,

$$\nu_L = |\hat{g} \cdot \boldsymbol{B} \mu_B + \sum_j A_H(j)\langle \boldsymbol{I}(j)\rangle|/h, \qquad (1)$$

where $\hat{g}$ is the anisotropic g tensor of the electrons, μ_B the Bohr magneton, and h the Planck constant. $A_H(j)$ and $\langle \boldsymbol{I}(j)\rangle$ are the hyperfine constant and the averaged nuclear spin for the jth element (^{69}Ga, ^{71}Ga, or ^{75}As), respectively. When the resonant condition is fulfilled, simultaneous irradiation of cw $\boldsymbol{B}_{rf}$ (at fixed f_{rf}) reduces $\langle \boldsymbol{I}(j)\rangle$ and modulates ν_L as given by Eq. (1). Figure 1(b) shows typical NMR spectra appearing in θ_K, which was detected at a fixed Δt ($= 640$ ps) and $\alpha = 4°$, with a field sweep rate of 5 mT/min. At each resonance condition for ^{69}Ga, ^{71}Ga, and ^{75}As, clear peaks and dips reflecting the resonance change of ν_L were observed [26].

In the following, we focus on ^{71}Ga as a target nucleus: Fig. 1(c) shows the ^{71}Ga NMR spectra in θ_K obtained with a sweep rate of 1 mT/min in the vicinity of the resonant magnetic field $(\Delta B = B - 0.630$ T$)$. The linewidth (FWHM) of ~ 1.1 mT was obtained for $\alpha = 4°$. Under the exact resonance condition for ^{71}Ga ($B = 0.630$ T), we measured θ_K in a time domain: Fig. 1(d) shows θ_K as a function of Δt with and without applying $\boldsymbol{B}_{rf}$. It is found from Fig. 1(d) that ν_L decreases from 1.28 to 0.96 GHz by applying $\boldsymbol{B}_{rf}$. Using the experimentally determined $\hat{g}$ ($g_{[001]} = -0.045$ and $g_{[110]} = -0.161$) in Eq. (1), the decrease of the nuclear field is evaluated to be 37% [27]. This indicates that the nuclear spin polarization of ^{71}Ga is fully depolarized and also those of ^{69}Ga and ^{75}As are partially reduced as a result of modulated steady-state configuration for the coupled electron-nuclear spin system [28,29].

We now describe an optically pump-probed NMR with pulsed $\boldsymbol{B}_{rf}$. After saturation of nuclear polarization by optical pumping, we applied a single pulse $\boldsymbol{B}_{rf}$ with a width of $t^{(rf)}$, during which ^{71}Ga nuclear spins process around the x' axis in a rotating frame at f_{rf}. This modulates $\langle \boldsymbol{I}(^{71}Ga)\rangle$, resulting in the change of ν_L according to Eq. (1). For the observation of the temporal $\langle \boldsymbol{I}(^{71}Ga)\rangle$, we fixed Δt at a point where the change in θ_K is approximately proportional to that of $\langle \boldsymbol{I}(^{71}Ga)\rangle$.

A gray-scale map in Fig. 2(a) displays the laboratory-time (t_{lab}) evolution of θ_K measured at $\Delta t = 640$ ps when a pulse $\boldsymbol{B}_{rf}$ ($0 < t^{(rf)} < 200$ μs) is applied at $t_{lab} = 0$. A clear periodic oscillation is observed as a function of $t^{(rf)}$. In Fig. 2(b), θ_K for $t^{(rf)} = 16$ μs is plotted as a function of t_{lab}. After the irradiation of pulse $\boldsymbol{B}_{rf}$, θ_K shows a discontinuous jump (defined as $\Delta\theta_K$) at $t_{lab} = 0$ and then recovers exponentially with a time constant of ~ 30 s. In Fig. 2(c), we plotted $\Delta\theta_K$ measured for $0 < t^{(rf)} < 200$ μs and 600 μs $< t^{(rf)} < 750$ μs by circles. These
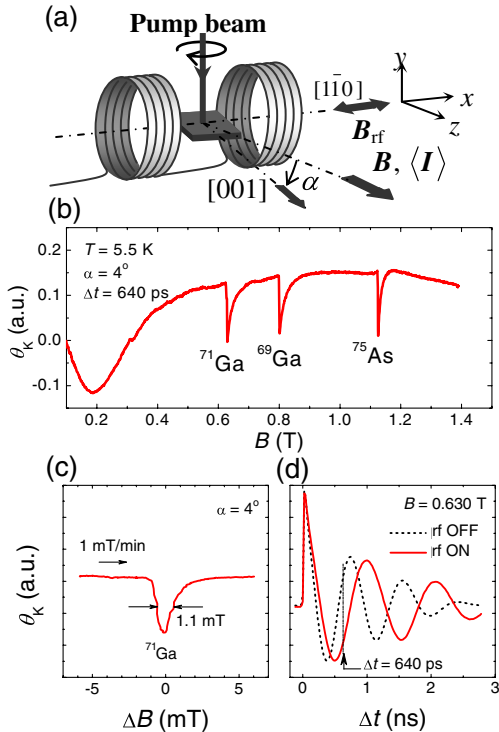

FIG. 1 (color online). (a) The experimental setup of NMR by optical pump-probe detection with a rf coil. (b) The NMR spectra appeared in TRKR signal: The data were obtained at $\Delta t = 640$ ps with $\boldsymbol{B}_{rf}$ at 8.18 MHz. (c) Close view of the NMR spectra (b) in the vicinity of ^{71}Ga resonance ($\Delta B = B - 0.630$ T) (d) The electron Larmor precession at $B = 0.630$ T with and without applying $\boldsymbol{B}_{rf}$.
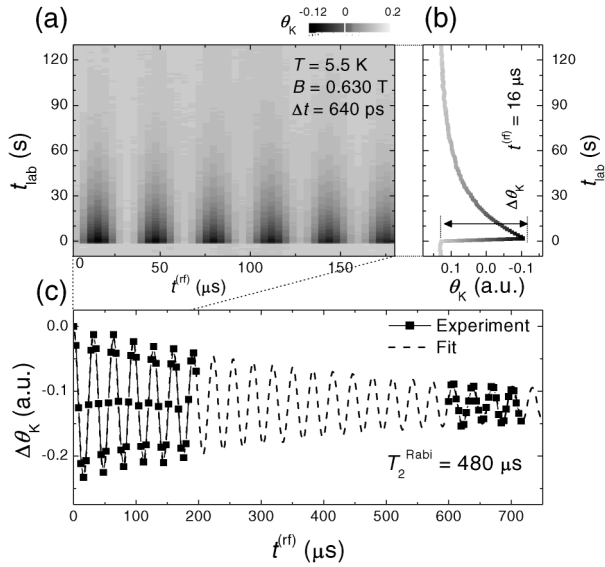
FIG. 2. Optically detected Rabi oscillation of ^{71}Ga: (a) gray-scale plot of TRKR signals (θ_K at $\Delta t = 640$ ps) when a pulse B_{rf} with $t^{(rf)}$ is applied at $t_{lab} = 0$ s. (b) θ_K for $t^{(rf)} = 16$ μs is plotted as a function of t_{lab}. (c) $\Delta\theta_K$ defined in (b) is plotted as a function of $t^{(rf)}$, representing the Rabi oscillation of ^{71}Ga. A solid curve is the fitted result.

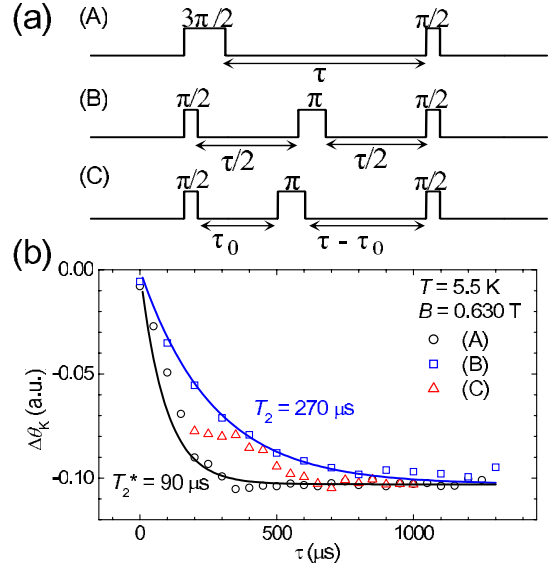

FIG. 3 (color online). (a) B_{rf} pulse sequences for observation of quantum coherence of nuclear spin (^{71}Ga) are shown. (b) The changes in TRKR signal $\Delta\theta_K$ after application of the pulse sequences (A), (B), and (C) plotted as a function of the time interval τ. The result of (B) (spin echo) gives the intrinsic coherence time T_2 of ^{71}Ga.

represent the quantum coherence of ^{71}Ga nuclear spins, i.e., Rabi oscillation. The data shown in Fig. 2(c) can be fitted by

$$\Delta\theta_K = A_0 \cos(2\pi\nu_{Rabi}t^{(rf)})\exp(-t^{(rf)}/T_2^{Rabi}) - 1, \quad (2)$$

as indicated by a solid curve, where A_0 is a constant. From the fit, the effective dephasing times of the Rabi oscillation $T_2^{Rabi} = 480$ μs and the Rabi frequency $\nu_{Rabi} = 31.35$ kHz are obtained, from which we can also estimate the amplitude $|B_{rf}|$ to be ~ 2 mT.

From the period of Rabi oscillation shown in Fig. 2(c), the durations for $\pi/2$, π, and $3\pi/2$ pulses are given as 8, 16, and 24 μs, respectively. By using these pulses, we performed local spin-echo measurements to evaluate the intrinsic coherence time T_2 of ^{71}Ga. Figure 3(a) shows the B_{rf} pulse sequences: In each sequence, the first $\pi/2$ or $3\pi/2$ pulse rotates $\langle I(^{71}Ga)\rangle$ down to the y' axis, while the last $\pi/2$ pulse (in phase) turns the remaining $\langle I(^{71}Ga)\rangle$ back to the initial direction (z axis) for the detection of the loss of $\langle I(^{71}Ga)\rangle$ as a change of ν_L or θ_K. The sequence (A) gives the effective coherence time T_2^* involving the inhomogeneous broadening which randomizes the phase information of ^{71}Ga spin precessions during the interval τ. The sequence (B) is the spin echo which provides T_2 by refocusing. In the sequence (C) we expect the refocusing effect only when the intervals τ_0 and $\tau - \tau_0$ are equal to each other. In Fig. 3(b), $\Delta\theta_K$ [defined in Fig. 2(b)] is plotted as a function of the interval τ. For the sequences (A) and (B), $\Delta\theta_K$ can be fitted by single exponential decay functions of τ, from which we read $T_2^* = 90$ μs and $T_2 = 270$ μs, respectively. $T_2^{Rabi} = 480$ μs, shown in Fig. 2(c), is in

good agreement with the relation $T_2^{Rabi} \sim 2T_2$ given by solving Bloch equations for the case $T_1 \gg T_2$, T_2^{Rabi}. In the sequence (C), $\Delta\theta_K$ is found to approach the result of sequence (B) at $\tau - \tau_0 = \tau_0$ ($= 200$ μs), as expected.

The dipole-dipole interaction among the nuclei [1] is expected to be the most relevant mechanism limiting the intrinsic T_2. One of the advantages of the optical pump-probe technique is that we can apply B at an angle with respect to the crystal axis of the sample. Here we examined the effect of the dipole-dipole interaction, especially the contribution of the first nearest nuclei ^{75}As. We performed a set of TRKR measurements with cw and pulse B_{rf} by setting the sample at $\alpha = 45°$. In Fig. 4(a), the cw-NMR signal of ^{71}Ga for $\alpha = 45°$ is shown. Compared to the result in Fig. 1(c) for $\alpha = 4°$, the line width (2.8 mT) becomes broader by a factor of 2.5. Figure 4(b) shows the Rabi oscillation for $\alpha = 45°$, in which the decay constant $T_2^{Rabi} \sim 220$ μs becomes also shorter than 480 μs for $\alpha = 4°$. By spin-echo measurements at $\alpha = 45°$ (not shown), we obtained $T_2 = 100$ μs and $T_2^* = 60$ μs, respectively, both of which are about $1/2 \sim 1/3$ of those for $\alpha = 4°$. This decrease of coherence by tilting B with respect to the crystalline axis of the sample can be understood by the enhanced dipole-dipole interaction: When the first nearest nuclei are taken into account and the flip-flop processes are neglected, the effective magnetic field B_{dd} due to the dipole-dipole interaction is proportional to $1 - 3\cos^2\theta$, where θ is the angle between B and the relative positions of neighboring two nuclei. When $\alpha \sim 0°$, i.e., $B \parallel [001]$, θ becomes 53.4° (magic angle) in a tetrahedral unit cell of GaAs and gives the minimum B_{dd}
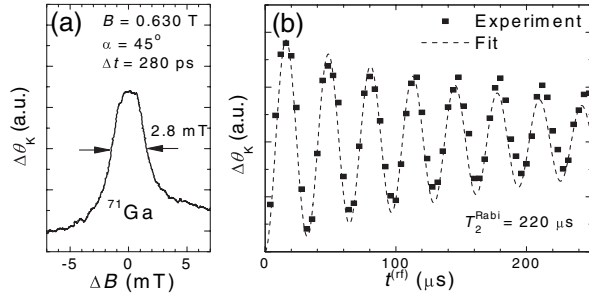
FIG. 4.   (a) The cw-NMR spectra of ^{71}Ga measured at $\alpha = 45°$ detected by TRKR. $\Delta B = B - 0.630$ T   and $\Delta t = 280$ ps. (b) The Rabi oscillation obtained by pulse NMR at $\alpha = 45°$ is plotted by closed circles. A solid curve is the fitted result.

contribution from the nearest neighbors, while for $\alpha = 45°$ B_{dd} induced by polarized ^{75}As nuclei dephase the nuclear spin of ^{71}Ga much more rapidly.

Finally, we comment on the dephasing mechanism. It is known that T_2^* is limited by the existence of inhomogeneous fields. In our system, however, nonuniformity of $\boldsymbol{B}$ or $\boldsymbol{B}_{rf}$ is probably not significant, since we observed NMR within a small volume of less than 0.1 μm thick and 40 μm diameter. Possible mechanisms responsible for dephasing in our system include the nonuniformity of the photoexcited electron density and the ensemble of different electronic states in a doped QW as well as the nonuniformity among the five QW layers.

In conclusion, we have demonstrated the quantum coherence of local nuclear spin polarization in semiconductor quantum wells which are successfully manipulated and detected by a TRKR technique combined with cw and pulsed rf magnetic field. Spin-echo measurements with programmed pulse sequences provided us the intrinsic coherence time of $\sim 10^{12}$ nuclei. The present approach will be applicable to the manipulation and detection of coherent dynamics of local nuclear spin in semiconductor nanostructures for future semiconductor quantum information technologies.

*Electronic address: oono@riec.tohoku.ac.jp
†Electronic address: ohno@riec.tohoku.ac.jp

[1] A. Abragam, *The Principle of Nuclear Magnetism* (Oxford University, Oxford, 1961).

[2] M. A. Nielsen and I. L. Chang, *Quantum Computation and Quantum Information* (Cambridge University Press, New York, 2000).
[3] B. E. Kane, Nature (London) **393**, 133 (1998).
[4] T. D. Ladd *et al.*, Phys. Rev. Lett. **89**, 017901 (2002).
[5] M. N. Leuenberger, D. Loss, M. Poggio, and D. D. Awschalom, Phys. Rev. Lett. **89**, 207601 (2002).
[6] G. Salis *et al.*, Phys. Rev. Lett. **86**, 2677 (2001).
[7] M. Poggio *et al.*, Phys. Rev. Lett. **91**, 207602 (2003).
[8] H. Sanada *et al.*, Phys. Rev. Lett. **94**, 097601 (2005).
[9] D. Gammon *et al.*, Science **277**, 85 (1997).
[10] A. K. Hüttel *et al.*, Phys. Rev. B **69**, 073302 (2004).
[11] K. Ono and S. Tarucha, Phys. Rev. Lett. **92**, 256803 (2004).
[12] *Optical Orientation*, edited by F. Meier and B. P. Zakharchenya (Elsevier, Amsterdam, 1984).
[13] G. Lampel, Phys. Rev. Lett. **20**, 491 (1968).
[14] S. E. Barrett, R. Tycko, L. N. Pfeiffer, and K. W. West, Phys. Rev. Lett. **72**, 1368 (1994).
[15] M. Krapf *et al.*, Solid State Commun. **78**, 459 (1991).
[16] D. Paget, G. Lampel, B. Sapoval, and V. I. Safarov, Phys. Rev. B **15**, 5780 (1977).
[17] V. K. Kalevich, V. D. Kul'kov, and V. G. Fleisher, Sov. Phys. Solid State **22**, 703 (1980); V. K. Kalevich, V. D. Kul'kov, and V. G. Fleisher, Sov. Phys. Solid State **23**, 892 (1981); M. Eickhoff, B. Lenzman, G. Flinn, and D. Suter, Phys. Rev. B **65**, 125301 (2002).
[18] J. M. Kikkawa and D. D. Awschalom, Science **287**, 473 (2000).
[19] M. Poggio and D. D. Awschalom, Appl. Phys. Lett. **86**, 182103 (2005).
[20] J. A. Marohn *et al.*, Phys. Rev. Lett. **75**, 1364 (1995).
[21] F. Jelezko *et al.*, Phys. Rev. Lett. **93**, 130501 (2004).
[22] T. Machida, T. Yamazaki, K. Ikushima, and S. Komiyama, Appl. Phys. Lett. **82**, 409 (2003).
[23] G. Yusa *et al.*, Nature (London) **434**, 1001 (2005).
[24] The sample and the sensor are thermally coupled by fixing them on a copper holder, and the sample is in direct contact with the He vapor ensuring that the heat load is removed during the measurements.
[25] D. Gammon *et al.*, Phys. Rev. Lett. **86**, 5176 (2001); R. K. Kawakami *et al.*, Science **294**, 131 (2001).
[26] In the NMR spectra, no quadrupolar splitting is observed. The splitting is known to be induced by an electric field gradient which interacts with the quadrupole moments [1]. Indeed, the quadrupolar splitting appears in other places of the same epilayer after the GaAs substrate was removed for transmission measurements. Thus the absence of quadrupole splitting is likely due to a lack of internal strain field created by some post-growth process in the present sample.
[27] If all nuclei are equally polarized, 22% reduction of the total nuclear field is expected by subtracting the counterpart of ^{71}Ga nuclei [12].
[28] H. Sanada *et al.*, Phys. Rev. B **68**, 241303 (2003).
[29] This is supported by the observation of slower change of ν_L upon application of $\boldsymbol{B}_{rf}$ in a time scale of ~ 100 s after the instantaneous decrease of ν_L due to the depolarization of ^{71}Ga.